6th European Conference on Computational Mechanics (ECCM 6)
7th European Conference on Computational Fluid Dynamics (ECFD 7)
11–15 June 2018, Glasgow, UK

A HIGHER-ORDER CONFORMAL-DECOMPOSITION FEM FOR NURBS-BASED GEOMETRIES

JAKOB W. STANFORD[1] AND THOMAS-PETER FRIES[2]

[1,2] Institute of Structual Analysis, Graz University of Technology
Lessingstraße 25/II, 8010 Graz, Austria
www.ifb.tugraz.at
[1]stanford@tugraz.at, [2]fries@tugraz.at

Key words: embedded domain methods, fictitious domain methods, higher-order FEM, NURBS, CAGD

Abstract. To bridge the gap between design and analysis, a new method which allows for the fully automatic and higher-order accurate analysis of NURBS-based geometries is presented. This method borrows ideas from fictitious domain methods, where the geometry is immersed into a non-body-fitted background mesh, but is able to produce a computational mesh that can be used for both classical FEM and fictitious domain methods, as shown in the numerical results. The key point is to transfer the B-rep geometry into an implicit representation using level-set functions and use this implicit description to reconstruct Lagrangian elements that accurately match the given domain boundary.

1 INTRODUCTION

In recent years there have been efforts to tighten the interplay between design-tools (i.e., CAD-software) and analysis-tools (i.e., FEM-software). Despite high efforts, this is still an active field of research with main open topics remaining. One of the main problems are the vastly different requirements for the geometry description. In CAD, even solid geometry is usually represented by means of their boundary (B-rep). In numerical simulations, however it is often required to have an explicit representation of the bulk domain. The bulk of the domain therefore has to be reconstructed. Even for simulations where a boundary-representation is sufficient for analysis (such as curved shells in FEM and in Isogeometric Analysis in the frame of the Boundary Element Method) the geometry discretization provided by CAD-systems is typically not directly suitable for analysis. Reasons can be ill-parametrization of surfaces (e.g., tensor product patches with collapsed edges) or the topic of trimmed geometries; as surveyed by Marussig and Hughes [1]. For a discussion of the gap between design and analysis, see the review papers of Shephard et. al [2] and Riesenfeld and co-workers [3] and the references cited herein. In practice these incompatibilities lead to a complete (re-) meshing of the geometry involved. On meshing of B-rep geometries, there is an extensive body of literature available and the interested reader is referred to the works of Frey, George, et al. [4, 5] as well as the review conducted by Owen [6] and the references in the recent publication by Fortunato and co-workers [7].

A promising alternative to mesh generation is provided by a class of methods denoted as embedded domain, immersed boundary or fictitious domain methods. These methods do not require a user-provided mesh. Instead, the domain of interest is embedded into an arbitrarily simple background mesh. This mesh generally does not conform to the boundaries of the computational domain in a sense that element-edges are aligned to match domain boundaries. The effort from generating a conforming mesh is shifted there to the integration of the weak form and the consideration of boundary conditions. Established immersed boundary methods include the works of Mittal [8], Parzivan and Düster [9], Noble and co-workers [10, 11] as well as Burman et al. [12] and many others.

The method presented in this contribution can be seen as a hybrid between fictitious domain (FD) methods and classical mesh generation in a sense, that it uses many of the concepts employed in fictitious domain methods, but is able to produce a mesh that can be used in the context of classical finite element methods as well as FD methods. The procedure can be outlined as followed: The domain of interest is embedded into a background mesh, then the B-rep description is converted into an implicit level-set description. This level-set data is used to decompose background elements intersecting the domain boundary into sub-elements which are aligned to the domain boundary with higher-order accuracy. These sub-elements can either be merged back into the background-mesh, generating a body-fitted mesh, or can serve as a mapping to provide a higher-order integration scheme for use in embedded methods. The presented method is based on a higher-order integration scheme proposed in [13] and the concept of the conformal-decomposition FEM [11], which was extended to higher-order in [14, 15, 16, 17] for implicit geometries.

2 PRELIMINARIES

2.1 Geometry and Domain Definition

CAD-systems most commonly use Non-Uniform Rational B-Splines (NURBS) for the parametrization of B-rep geometries. For an in-depth discussion of NURBS, the reader is referred to the works [18, 19]. NURBS are piecewise smooth functions with typically higher-order continuity across knot spans (which may be interpreted as the ”elements” in Isogeometric Analysis). It is later seen that the consideration of the locations with reduced continuity is crucial for a consistent higher-order remeshing of the domain. Therefore in this work, all NURBS are split at the entries in the associated knot-vector into rational Beziér-curves $\mathbf{\Gamma}(\upsilon) = [\Gamma_x(\upsilon),\, \Gamma_y(\upsilon)]^\intercal : \mathbb{R} \rightarrow \mathbb{R}^2$.

In the present work, the domain of interest is described by a set of NURBS (or rational Beziér-curves) forming one or more closed loops, denoted herein as curve segments for brevity. The segments are aligned in a way that the curve's normal vector $\boldsymbol{n}(\upsilon) = [\Gamma_{y,u}(\upsilon),\, -\Gamma_{x,u}(\upsilon)]^\intercal$ is pointing outwards the domain of interest. This approach allows the definition of inclusions, can be extended to three dimensions and is consistent with the specification of trimmed NURBS in the IGES standard [20].

2.2 Level-Set Data from Beziér-Curves

In general, level-set functions [21, 22] allow the representation of a domain Ω via an inequality:

$$\Omega = \{\boldsymbol{x} \,|\, \phi(\boldsymbol{x}) \geq 0\} \qquad \boldsymbol{x} \in \mathbb{R}^{\{2,3\}}. \tag{1}$$

The level-set function $\phi(\boldsymbol{x})$ therefore must be

$$\phi(\boldsymbol{x}) \begin{cases} > 0 & \forall \boldsymbol{x} \in \Omega, \\ = 0 & \forall \boldsymbol{x} \in \partial\Omega, \\ < 0 & \text{otherwise.} \end{cases} \tag{2}$$

One such function to satisfy these properties is the signed-distance function

$$\phi(\boldsymbol{x}) = \pm \min_{\forall \boldsymbol{x}^\star \in \partial\Omega} \|\boldsymbol{x} - \boldsymbol{x}^\star\|, \tag{3}$$

which returns the distance from $\boldsymbol{x}$ to the closest point on the boundary, multiplied by a sign based on the direction of the normal vector at that point. In the case of Beziér-curves it is useful differentiate between the level-set function that returns the distance to the extension of the curve

$$\phi_{\Gamma,i}(\boldsymbol{x}) = \pm\min \|\boldsymbol{x} - \boldsymbol{\Gamma}_i(\upsilon)\| \qquad \upsilon \in \mathbb{R} \;, \tag{4}$$

and the one that respects the curves' boundaries by only considering $\boldsymbol{x}^\star$ in the interior of the curve

$$\hat{\phi}_{\Gamma,i}(\boldsymbol{x}) = \pm\min \|\boldsymbol{x} - \boldsymbol{\Gamma}_i(\upsilon)\| \qquad \upsilon \in [0,1] \;. \tag{5}$$

Furthermore it is useful to define level-sets to the distance of the curve's ends:

$$\phi_{\partial\Gamma,i,1}(\boldsymbol{x}) = \langle \boldsymbol{x} - \boldsymbol{P}_1, \boldsymbol{P}_2 - \boldsymbol{P}_1 \rangle \tag{6}$$

$$\phi_{\partial\Gamma,i,2}(\boldsymbol{x}) = \langle \boldsymbol{x} - \boldsymbol{P}_n, \boldsymbol{P}_{n-1} - \boldsymbol{P}_n \rangle, \tag{7}$$

where $\langle\cdot,\cdot\rangle$ denotes the scalar product and $\boldsymbol{P}_i$ coordinates of the curves' control polygon. See Figure 1 for a visualization of these level-sets. While $\phi_{\Gamma,i}(\boldsymbol{x})$, $\phi_{\partial\Gamma,i,1}(\boldsymbol{x})$ and $\phi_{\partial\Gamma,i,2}(\boldsymbol{x})$ may be used for the decomposition described in Sec. 3, $\hat{\phi}_{\Gamma,i}(\boldsymbol{x})$ on the other hand can be used to describe the domain in the sense of Eq. (1) by choosing the level-set with the minimal absolute value:

$$\phi_\Omega(\boldsymbol{x}) = \min\{|\hat{\phi}_{\Gamma,i}(\boldsymbol{x})|\} \cdot \text{sign}\left(\min\{\hat{\phi}_{\Gamma,i}(\boldsymbol{x})\}\right). \tag{8}$$

A treatment for the situation that multiple $\hat{\phi}_{\Gamma,i}(\boldsymbol{x})$ are of the same magnitude, but different sign was proposed in [23]. Note, that the resulting level-set function is not suitable for decomposing the background mesh, since its zero level-set is generally not smooth. This is because the corresponding NURBS also features points of reduced continuity across the knot spans and this is naturally reflected in a reduced continuity of the implicit level-set function. Of course, the overall continuity of the level-set function is of the same order than of the underlying NURBS.

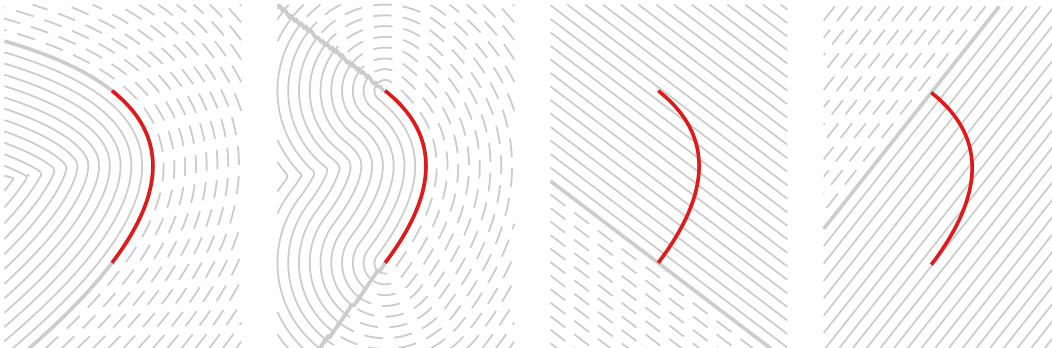

(a) $\phi_{\Gamma,i}(\boldsymbol{x})$ (b) $\hat{\phi}_{\Gamma,i}(\boldsymbol{x})$ (c) $\phi_{\partial\Gamma,i,1}(\boldsymbol{x})$ (d) $\phi_{\partial\Gamma,i,2}(\boldsymbol{x})$

Figure 1: Different level-sets associated with the same knot span.

2.3 Conformal-Decomposition for Smooth Level-Set Data

Conformal decomposition is the process where background elements intersecting the boundary are decomposed in a way that the resulting sub-elements are conforming to the boundary. The background-element-wise procedure follows closely the outline in [13, 14, 15] and is sketched as follows: 1) Evaluate the level-set function at all element nodes. 2) Determine if the background element is cut. 3) Identify the topological cut situation. 4) Depending on the cut scenario, find the roots of the level-set function along the element edges. 5) Determine the inner nodes of an interface element by again finding roots of the level-set function. 6) With the interface element at hand, define a mapping for the sub-elements into the cut background element. For an overview of this procedure, see Fig. 2. In case during step (3) no valid cut situation is found, the background element will be adaptively refined as needed. The adaptive process does not introduce hanging nodes and therefore poses no difficulties in the following mesh generation.

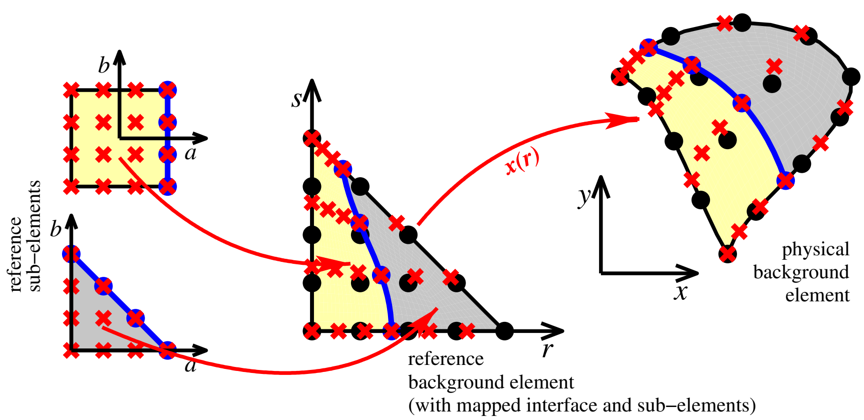

Figure 2: Overview of the general conformal decomposition process.

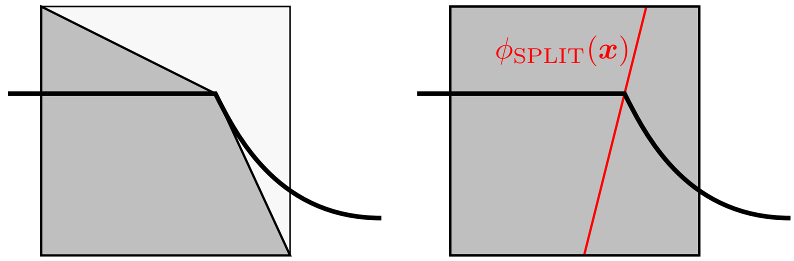

(a) (b)

Figure 3: Different alternatives for considering corners in the boundary.

3 CONFORMAL DECOMPOSITION OF BEZIÉR-CURVES

As the procedure outlined in the previous section requires level-set data to be sufficiently smooth, and since $\phi_\Omega(\boldsymbol{x})$ generally does not fulfill this property, the decomposition must use $\phi_{\Gamma,i}(\boldsymbol{x})$ instead. This requires a slight adaption of the procedure: First, before decomposition it must be ensured that points of reduced continuity (such as kinks, corners and, more general, across knot spans, i.e., directly at the knots) will—after decomposition—coincide with corners of the resulting sub-elements. Second, when decomposing using $\phi_{\Gamma,i}(\boldsymbol{x})$, it is desired only to decompose those parts of each $\phi_{\Gamma,i}(\boldsymbol{x})$ which are also part of the actual domain boundary.

3.1 Proper Consideration of Kinks and Corners

For those places with reduced continuity, i.e., at knots (where corners and kinks may occur or other points with reduced continuity), two alternatives are proposed.

(a) One option is to simply move nodes of the background mesh onto those special points. The advantage is that the resulting mesh does not introduce hanging nodes. The mesh manipulation may be smoothed out over the domain, e.g., to avoid local flipping of elements.

(b) Another possibility is to split background elements containing corners of the boundary. For that, the level-set

$$\phi_{\mathrm{SPLIT}}(\boldsymbol{x}) = \phi_{\partial\Gamma,i,1}(\boldsymbol{x}) \pm \phi_{\partial\Gamma,j,2}(\boldsymbol{x}) \tag{9}$$

is used to decompose the background element. This option may be useful for applications where the background mesh can not be moved.

Fig 3 demonstrates the two different options.

3.2 Local Decomposition

Because $\phi_{\Gamma,i}(\boldsymbol{x})$ is a *signed* distance function, its zero level-set can only be an unbounded curve. A decomposition of the whole background mesh using all $\phi_{\Gamma,i}(\boldsymbol{x})$ would not only result in unnecessarily decomposed elements, but would also lead to undesired

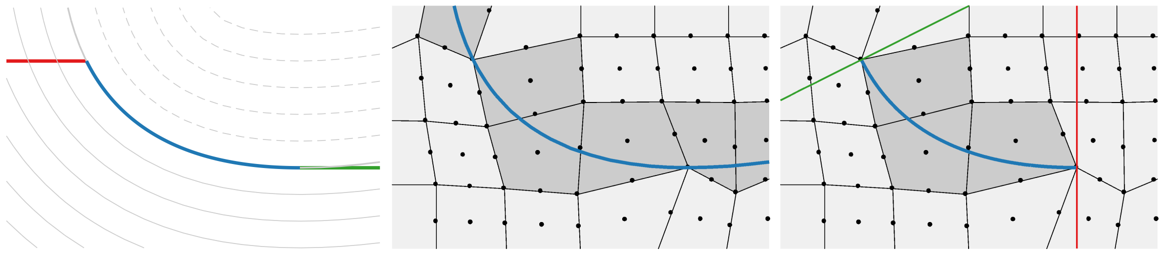

(a) (b) (c)

Figure 4: Comparison of regular decomposition (b) and bounded decomposition (c) of the curve segment in (a). Elements shaded gray would be decomposed by $\phi_{\Gamma,i}(\boldsymbol{x})$ belonging to the blue curved segment.

elements in case two curves cross each other tangentially. Therefore it is essential to only decompose a background element for a given $\phi_{\Gamma,i}(\boldsymbol{x})$ if the element would be cut by the corresponding $\boldsymbol{\Gamma}_i(\upsilon)$ as well. See Fig. 4 for a visual explanation. Herein this is denoted as *local decomposition*. To accomplish this, we make use of the fact that due to the measures described in Sec. 3.1 a background element is either totally intersected by a $\boldsymbol{\Gamma}_i(\upsilon)$ or not all.

In general, using level-set data, an element Ω^{el} is said to be cut if

$$\min \phi_{\Gamma,i}(\boldsymbol{x}) \cdot \max \phi_{\Gamma,i}(\boldsymbol{x}) < 0 \quad \forall \boldsymbol{x} \in \Omega^{\text{el}}. \tag{10}$$

However, to accomplish a bounded decomposition only elements fulfilling

$$\min \phi_{\Gamma,i}(\boldsymbol{x}) \cdot \max \phi_{\Gamma,i}(\boldsymbol{x}) < 0 \quad \forall \boldsymbol{x} \in \{\boldsymbol{x} \,|\, \phi_{\partial\Gamma,i,1}(\boldsymbol{x}) > 0\,,\, \phi_{\partial\Gamma,i,2}(\boldsymbol{x}) > 0\}. \tag{11}$$

are decomposed. Essentially, this only considers level-set values of locations $\boldsymbol{x}$ which are projecting on the interior of the curve.

4 NUMERICAL EXAMPLES

4.1 Model Problem

In this section the following model problem shall be considered:

$$\Delta u(\boldsymbol{x}) = -f(\boldsymbol{x}) \quad \forall \boldsymbol{x} \in \Omega \tag{12}$$

$$u(\boldsymbol{x}) = \tilde{u}(\boldsymbol{x}) \quad \forall \boldsymbol{x} \in \partial\Omega \tag{13}$$

To facilitate the measurement of errors, a manufactured solution was created based on $u(\boldsymbol{x}) = \cos(2\pi(2x + 2y)) + \sin(4\pi x)$. For comparison we compare the full CD-FEM approach, where a classical higher-order mesh is being created, with an embedded-domain approach.

In the FDM employed herein, we use the shape functions provided by the background mesh and only integrate over the part that is inside our domain of interest using the integration points provided by the decomposed background elements. In contrast, in the CD-FEM approach, the conforming mesh, resulting from the decomposition, is being used for the construction of the approximation space.

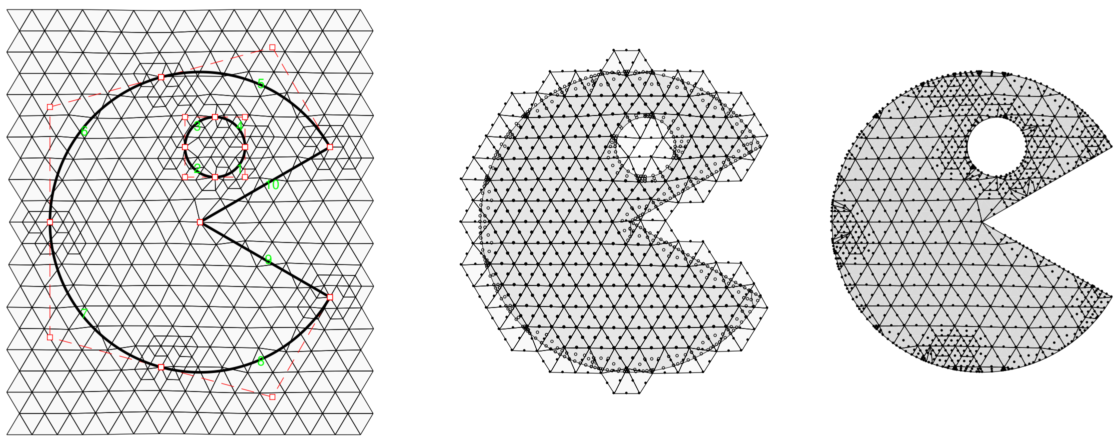

(a) Initial background mesh and B-rep as Beziér-curves

(b) Background mesh for the embedded-domain variant (light gray) and the sub-elements used for integration.

(c) Conforming mesh used for the CD-FEM variant.

Figure 5: Meshes for the coarsest background-element size h used in the study.

To apply boundary conditions in the FDM, the symmetric variant of the Nitsche method was applied, as summarized in [24]. In order to avoid an ill-conditioned system of equations, nodes close to $\partial\Omega$ were slightly moved away from the boundary, as discussed in [17].

4.2 Results

For both variants, a convergence study was conducted, measuring the relative L_2-error in the primal variable

$$\varepsilon_{u,L_2} = \frac{\|u^{ex} - u^h\|_{L_2}}{\|u^{ex}\|_{L_2}} \tag{14}$$

as well as the relative error in the approximated area

$$\varepsilon_{\text{Area}} = \frac{|A^{\text{ref}} - A^h|}{A^{\text{ref}}} \ . \tag{15}$$

In Fig. 5, the coarsest meshes generated during the study are shown. Fig. 6 summarizes the results for both variants. Comparing the behavior of $\varepsilon_{\text{Area}}$ for both variants, one can see similar results. Since both variants use the same integration points this is as expected. Comparing ε_{u,L_2}, both variants show higher-order rates of convergence. However, it can be found that the CD-FEM approach gives rates of optimal order, whereas this is less obvious for the FD-approach. In particular, the FD-approach yields considerably higher condition numbers κ_{est} for the stiffness matrix, which may explain the inferior results in ε_{u,L_2} compared to the CD-FEM. It is thus found that the concept of manipulating the background mesh to avoid ill-conditioning is considerably more efficient for the CD-FEM than for the fictitious domain method. Hence, additional stabilization terms as suggested in the CutFEM [25] are recommended for FDMs.

5 CONCLUSIONS AND OUTLOOK

A higher-order Conformal-Decomposition FEM for NURBS-based geometries was presented, being a hybrid between a classical approach to meshing and what is customary in embedded domain methods. The new method works by embedding the geometry into a higher-order background mesh, converting the B-rep geometry into an implicit level-set description and then decomposing background elements. That is, reconstructing sub-elements which are accurately aligned to consider the geometry boundary. For further analysis, the resulting sub-elements can then either be used to create a mesh for use in a classical p-FEM setting using Lagrangian elements. Alternatively the sub-elements can provide a higher-order integration rule for embedded-domain methods. Both options have been demonstrated to work in a numerical study where higher-order rates of convergence in the L_2-norm could be achieved.

Regarding the extension to three dimensions, the following remark holds: Although the simple concept of separating the background elements along discontinuities, can be extended to three dimensions in principle, one needs to consider the additional effort resulting from the fact that for a higher-order accurate analysis, one needs to properly consider *all* points and lines of reduced continuity. In the case of NURBS-surfaces, this includes all ”knot-lines” (iso-lines of the knots), which for the case of quadratic NURBS, are usually are geometrically C^1-continuous. That said, it is questionable, whether this approach in 3D still can beat traditional approaches to meshing such geometries in terms of implementation effort, robustness and accuracy.

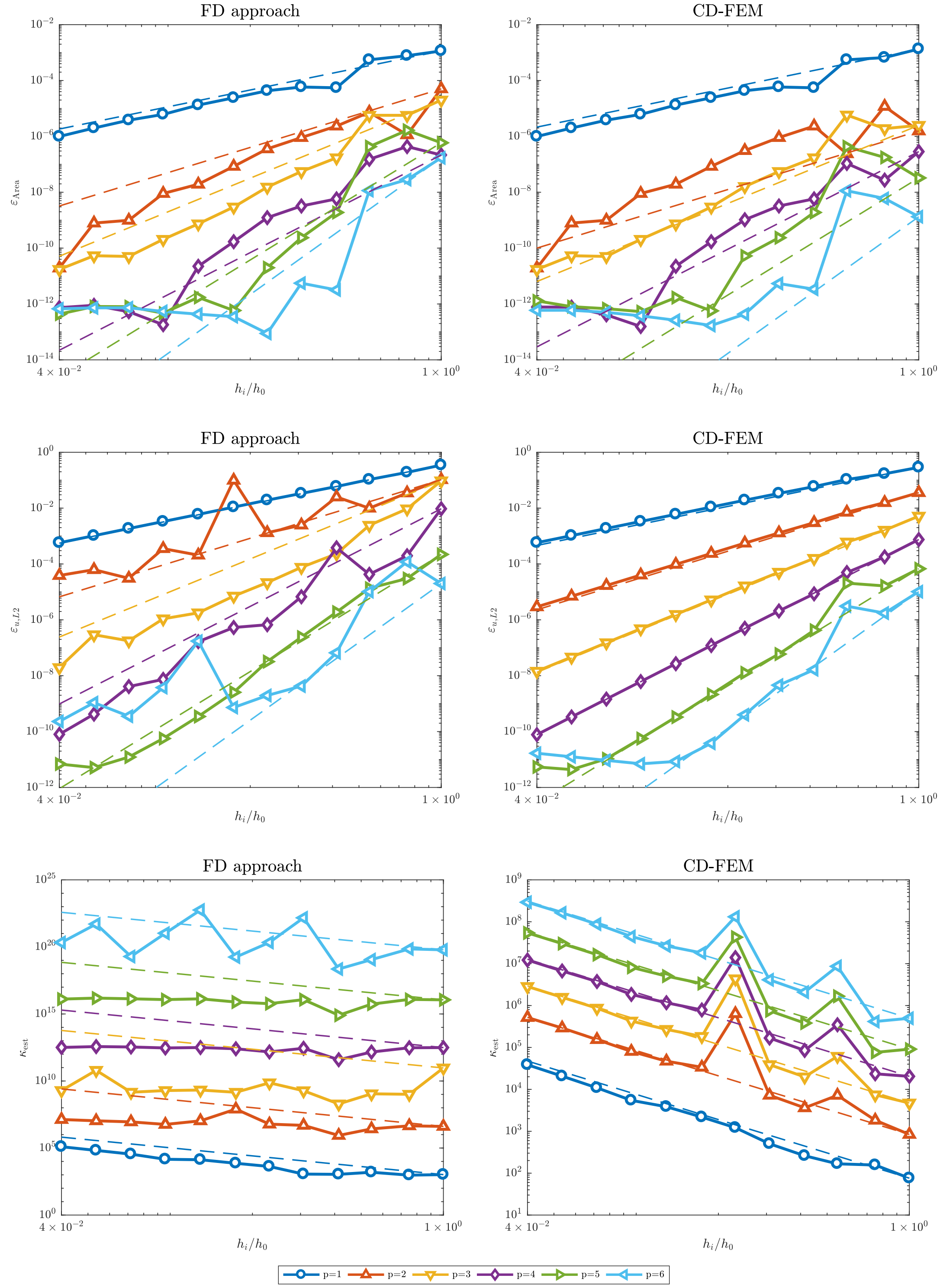

Figure 6: Results of the convergence study. Dashed lines indicate the expected slope for the corresponding Ansatz-order.

REFERENCES

[1] B. Marussig, T. J. R. Hughes, A review of trimming in isogeometric analysis: Challenges, data exchange and simulation aspects. *Archive Comp. Mech. Engrg.*, 2017.

[2] M. S. Shephard, M. W. Beall, R. M. O'Bara, B. E. Webster, Toward simulation-based design. *Finite Elements in Analysis and Design*, **40**(12), 1575–1598, 2004.

[3] R. F. Riesenfeld, R. Haimes, E. Cohen, Initiating a cad renaissance: Multidisciplinary analysis driven design: Framework for a new generation of advanced computational design, engineering and manufacturing environments. *Comp. Methods Appl. Mech. Engrg.*, **284**, 1054–1072, 2015.

[4] P. Frey, P.-L. George, *Mesh generation: Application to finite elements*. John Wiley & Sons, Chichester, 2008.

[5] P. L. George, *Automatic mesh generation: Application to finite element methods*. John Wiley & Sons, Chichester, 1992.

[6] S. J. Owen. A survey of unstructured mesh generation technology. In *International Meshing Roundtable*, 2000.

[7] M. Fortunato, P.-O. Persson, High-order unstructured curved mesh generation using the winslow equations. *Journal of Computational Physics*, **307**, 1–14, 2016.

[8] R. Mittal, G. Iaccarino, Immersed Boundary Methods. *Annu. Rev. Fluid Mech*, **37**(1), 239 – 261, 2005.

[9] J. Parvizian, A. Düster, E. Rank, Finite cell method. *Comput. Mech.*, **41**(1), 121–133, 2007.

[10] D. R. Noble, E. P. Newren, J. B. Lechman, A conformal decomposition finite element method for modeling stationary fluid interface problems. *Int. J. Numer. Methods Fluids*, **63**(6), 725–742, 2010.

[11] R. M. J. Kramer, D. R. Noble, A conformal decomposition finite element method for arbitrary discontinuities on moving interfaces. *International Journal for Numerical Methods in Engineering*, **100**(2), 87–110, 2014.

[12] E. Burman, P. Hansbo, Fictitious domain finite element methods using cut elements: I. a stabilized lagrange multiplier method. *Comp. Methods Appl. Mech. Engrg.*, **199**(41-44), 2680–2686, 2010.

[13] T. Fries, S. Omerović, Higher-order accurate integration of implicit geometries. *Internat. J. Numer. Methods Engrg.*, **106**(5), 323–371, 2016.

[14] S. Omerović, T.-P. Fries, Conformal higher-order remeshing schemes for implicitly defined interface problems. *Internat. J. Numer. Methods Engrg.*, **109**(6), 763–789, 2016.

[15] T. P. Fries, S. Omerović, D. Schöllhammer, J. Steidl, Higher-order meshing of implicit geometries - part I: Integration and interpolation in cut elements. *Comp. Methods Appl. Mech. Engrg.*, **313**, 759–784, 2017.

[16] T. Fries, D. Schöllhammer, Higher-order meshing of implicit geometries, part II: Approximations on manifolds. *Comp. Methods Appl. Mech. Engrg.*, **326**, 270–297, 2017.

[17] T.-P. Fries, Higher-order conformal decomposition FEM (CDFEM). *Comp. Methods Appl. Mech. Engrg.*, 2017.

[18] L. Piegl, W. Tiller, *The NURBS book*. Springer, Berlin, 1997.

[19] C. D. Boor, *A practical guide to splines, revised edition*, Vol. 27 of *Applied Mathematical Sciences*. Springer, Berlin, 2001.

[20] US Product Data Association. Initial Graphics Exchange Specification IGES 5.3, ANS US PRO. IPO-100-1996, ANSI Approved September 23, 1996.

[21] S. Osher, R. P. Fedkiw, Level set methods: An overview and some recent results. *J. Comput. Phys.*, **169**(2), 463–502, 2001.

[22] J. A. Sethian, A fast marching level set method for monotonically advancing fronts. *Proceedings of the National Academy of Sciences*, **93**(4), 1591–1595, 1996.

[23] J. W. Steidl, T.-P. Fries. Automatic Conformal Decomposition of Elements cut by NURBS. In *Proceedings of the VII ECCOMAS Congress*, 2016.

[24] S. Fernández-Méndez, A. Huerta, Imposing essential boundary conditions in mesh-free methods. *Comp. Methods Appl. Mech. Engrg.*, **193**(12-14), 1257–1275, 2004.

[25] E. Burman, P. Hansbo, M. G. Larson, A stabilized cut finite element method for partial differential equations on surfaces: The laplace–beltrami operator. *Comp. Methods Appl. Mech. Engrg.*, **285**, 188 – 207, 2015.